

Durham Research Online

Deposited in DRO:

29 June 2016

Version of attached file:

Accepted Version

Peer-review status of attached file:

Peer-reviewed

Citation for published item:

Caldwell, S. and Johnson, D. and Didsbury, M. and Murray, B. and Wu, J.J. and Przyborski, S. and Cameron, N.R. (2012) 'Degradable emulsion-templated scaffolds for tissue engineering from thiol-ene photopolymerisation.', *Soft matter.*, 8 (40). pp. 10344-10351.

Further information on publisher's website:

<http://dx.doi.org/10.1039/c2sm26250a>

Publisher's copyright statement:

Additional information:

Use policy

The full-text may be used and/or reproduced, and given to third parties in any format or medium, without prior permission or charge, for personal research or study, educational, or not-for-profit purposes provided that:

- a full bibliographic reference is made to the original source
- a [link](#) is made to the metadata record in DRO
- the full-text is not changed in any way

The full-text must not be sold in any format or medium without the formal permission of the copyright holders.

Please consult the [full DRO policy](#) for further details.

Degradable Emulsion-templated Scaffolds for Tissue Engineering from Thiol-Ene Photopolymerisation

Sally Caldwell^{a,b}, David W. Johnson^{a,b}, Matthew P. Didsbury^{a,b}, Bridgid A. Murray^{b,d}, Jun Jie Wu^{b,c}, Stefan A. Przyborski^{b,d,e}, Neil R. Cameron^{*a,b}

^a Department of Chemistry, Durham University, South Road, Durham, DH1 3LE, U.K. Email: n.r.cameron@durham.ac.uk.

^b Biophysical Science Institute, Durham University, South Road, Durham, DH1 3LE, U.K.

^c School of Engineering and Computer Sciences, Durham University, South Road, Durham, DH1 3LE, UK

^d School of Biological and Biomedical Science, Durham University, South Road, Durham, DH1 3LE, UK

^e Reinnervate Ltd, NETPark Incubator, Thomas Wright Way, Sedgefield, County Durham, TS21 3FD, UK

Abstract

Emulsion templating has been used to prepare highly porous polyHIPE materials by thiol-ene photoinitiated network formation. Commercially available multifunctional thiols and acrylates were formulated into water-in-oil high internal phase emulsions (HIPEs) using an appropriate surfactant, and the HIPEs were photo-cured. The temperature of the HIPE aqueous phase was found to influence the morphology of the resulting materials. In agreement with previous work, a higher aqueous phase temperature (80°C) gave rise to a larger mean void and interconnect diameter. The influence of temperature on morphology was found to be reduced at higher porosity, but still significant. The Young's modulus of the porous materials was shown to be related to the functionality of the acrylate comonomer used. A mixture of penta- and hexa-acrylate gave rise to a 100-fold increase in modulus, compared to an analogous tri-functional acrylate. The materials could be functionalised conveniently by addition of mono-acrylates or thiols to the organic phase of the precursor HIPE. Degradation was observed to occur at a rate depending on the degradation conditions. Under cell culture conditions at 37 °C, 19% mass loss occurred over 15 weeks. The scaffolds were found to be capable of supporting the growth of keratinocytic cells (HaCaTs) over 11 days in culture. Some penetrative in-growth of the cells into the scaffold was observed.

Introduction

Emulsion templating is a convenient method to prepare highly porous polymeric materials with well-defined morphology¹⁻⁶. The process involves preparing a high internal phase emulsion (HIPE), i.e. an emulsion with an internal (droplet) phase that comprises more than 74% of the total emulsion volume⁷, and then solidifying the external (non-droplet) phase. In this manner, the emulsion droplets template the pores within a solid foam, and the porosity is simply determined by the HIPE internal volume phase fraction (ϕ). In the vast majority of cases, on polymerisation the HIPE droplets connect with all of their neighbours to yield, on removal of the droplet phase, a highly interconnected, permeable material of low bulk density once the droplet phase has been removed. These materials, commonly termed polyHIPEs, have been prepared from a wide range of chemistries, including polystyrene^{8, 9}, polystyrene derivatives¹⁰⁻¹³, poly(meth)acrylates¹⁴⁻¹⁷, polyacrylamides¹⁸⁻²⁰, poly(ether sulfone)s²¹, norbornenes²², poly(propylene fumarate)²³, dicyclopentadiene^{24, 25}, polysaccharides²⁶ and proteins^{27, 28}.

In most cases, polyHIPE materials are produced by thermal curing using free radical initiation, however recently there has been significant interest in the use of photopolymerisation as a curing method²⁹⁻³¹. Photopolymerisation is typically a very rapid process (complete curing in seconds is common), which allows the use of less stable HIPEs than in thermal curing. This increases the range of precursor materials available for polyHIPE preparation. In previous work we demonstrated that thiol-ene and thiol-yne photopolymerisation,

employing commercially available multifunctional thiols with either multifunctional acrylates or alkynes, can also be employed for the preparation of polyHIPE materials³². These methods yield well-defined thiol-ene/yne network polyHIPE materials with mechanical properties dependent on the extent of crosslinking.

Thiol-ene networks produced from components such as those in Scheme 1 are essentially crosslinked aliphatic polyesters. This imparts (bio)degradability to these materials and opens up the prospect of their use as scaffolds for tissue engineering. Emulsion-templated scaffolds have previously been explored as scaffolds for tissue engineering^{26-28, 33-41}, however in almost all cases the materials used contain significant amounts of non-degradable carbon backbone polymer chains, potentially limiting their clinical applicability (the exception are enzymatically crosslinked gelatin scaffolds developed by Barbetta et al.²⁸). In addition, non-degradable styrene-based polyHIPEs have been used extensively for *in vitro* 3D cell culture⁴²⁻⁴⁵, but these scaffolds similarly are not suitable for *in vivo* applications.

Although thiol-ene polyHIPE materials have already been described, their suitability as scaffolds for tissue engineering has not been demonstrated. Key parameters to establish are an appropriate pore size, biodegradability and biocompatibility. The interconnect and void diameters of previously reported materials³² ranged from 4-13 μm and from 15-20 μm respectively. The

temperature of the emulsion aqueous phase was therefore increased in an attempt to increase the mean void diameter⁴⁶ to a value that is more suitable for cell infiltration (at least 50 μm). Biodegradability is also a requirement of tissue engineering scaffolds consequently the degradation of the scaffolds under different conditions was studied. The use of acrylates of different levels of functionality to influence the scaffold mechanical properties was also explored, since stiffness is known to influence the ability of cells to adhere to and proliferate on substrates⁴⁷. *In situ* chemical functionalisation using mono-thiols and acrylates was investigated. Finally, scaffold biocompatibility was investigated by exploring the ability of the scaffolds to support the growth of immortalised human keratinocytes.

2. Experimental Section

2.1 Materials

The monomers trimethylolpropane tris(3-mercaptopropionate) (trithiol), trimethylolpropane triacrylate (TMPTA) and dipentaerythritol penta/hexa-acrylate (DPEHA), the photoinitiator (a blend of diphenyl(2,4,6-trimethylbenzoyl)phosphine oxide / 2-hydroxy-2-methylpropiophenone), chloroform, fluorescein *o*-acrylate, 1,1,1,3,3,3-hexafluoroisopropyl acrylate (HFiPA) and 2,2,2-trifluoroethanthiol (fluorothiol) were obtained from Sigma Aldrich and used as supplied. The surfactant Hypermer B246, obtained from Croda, is a triblock copolymer of polyhydroxystearic acid and polyethylene glycol and was used as supplied. Alvetex® 3D cell culture scaffolds were obtained from Reinnervate Ltd.

2.2 PolyHIPE Preparation

The procedure was based on the work by Lovelady et al.³² An oil phase consisting of trithiol, TMPTA or DPEHA, chloroform, surfactant Hypermer B246 (0.46g, 2.5% w/w of oil phase) and photoinitiator (0.7 ml, 5% v/v of oil phase) was added to a two-necked round bottomed flask. The oil phase was stirred continuously at 380 rpm using a D-shaped polytetrafluoroethylene (PTFE) paddle attached to an overhead stirrer. An aqueous phase of deionised water heated to the correct temperature was added drop-wise to the oil phase to form a HIPE. The volumes of the monomers, chloroform and deionised water along with the temperatures are given in Table S1. Once all

the aqueous phase had been added, the HIPE was stirred for a further five minutes. The HIPE was then poured into a cylindrical PTFE mould with a diameter of 50 mm and a depth of either 17 mm or 30 mm. The moulds were secured between two glass plates and passed under a UV irradiator (Fusion UV Systems Inc. Light Hammer® 6 variable power UV curing system with LC6E benchtop conveyor) eight to twelve times on each side at a belt speed of 4.0 m.min⁻¹. The resulting polyHIPE was then washed in acetone and dried in a vacuum oven at 55°C overnight.

2.2 *In Situ* Chemical Functionalisation

PolyHIPEs were prepared as described in section 2.1. Model functional molecules were added to the HIPE organic phase as follows: fluorescein o-acrylate at 1 and 2 mol% of the acrylate content; HFiPA at 1, 2 and 5 mol% of the acrylate content; fluorothiol at 1 and 2 mol% of the thiol content.

2.3 Characterisation

2.3.1 Scanning Electron Microscopy

The polyHIPE morphologies were investigated using a Philips/FEI XL30 SEM operating at 25kV. Samples were mounted on carbon fibre pads attached to aluminium stubs and coated with gold using an Edwards Pirani 502 sputter coater. The image analysis software Image J⁴⁸ was used to calculate the average void diameter. Fifty voids were randomly chosen from a scanning electron microscopy (SEM) image of the sample and the diameters measured.

Void diameters measured in this way underestimate the true value as the voids are unlikely to be exactly bisected. Therefore a statistical correction factor was used to account for this underestimate⁴⁶.

2.3.2 Mercury Intrusion Porosimetry

Mercury intrusion porosimetry analysis was performed using a Micromeritics AutoPore IV. Intrusion and extrusion mercury contact angles of 130° were used. Penetrometers with a stem volume of 1.19 ml and a bulb volume of 4.25 ml were used. The intrusion volume always comprised between 30% and 65% of the stem volume. Intrusion pressures for the polyHIPE did not exceed 1600 psi.

2.3.3 Elemental Analysis

Sulphur and fluorine content were evaluated using a Dionex DX-120 Ion Chromatograph. The DX-120 is an integrated, preconfigured ion chromatograph (IC) that performs isocratic IC separations using digital conductivity detection. Powdered polyHIPE samples were prepared for sulphur and fluorine analysis by freezing in liquid nitrogen and pulverising with a pestle and mortar.

2.3.4 Solid-State ¹³C NMR Spectroscopy

Solid state ^{13}C NMR spectra were recorded using a Varian VNMRs 400 spectrometer. The spectra were obtained at a frequency of 100.562 MHz using the direct excitation experiment with proton decoupling. A 90° excitation pulse was used with a 3s recycle delay at a spin rate of 6800 Hz. At least 2000 repetitions were accumulated with an acquisition time of 20 ms. Spectra were obtained using on-board Varian NMR software.

Solid-state ^{13}C NMR: (100 MHz), δC ppm = 172.5 [-COO-], 130.4 [-C=C-], 64.7 [-C-O-], 43.7 [-C-S-], 35.2 [CR₄], 28.7, 20.6 [-S-CH₂-CH₂-], 8.3 [CH₃].

2.3.5 Mechanical Testing

Dumbbell-shaped samples of 3 mm depth were cut using a scalpel and a metal dumbbell-shaped tensile specimen template. The samples were then subjected to tensile testing using an Instron 5565 Materials Testing System. All samples were mounted very carefully in the tensile grips without any damage to the gripping part of the samples. All samples were tensile loaded uniaxially to break at a constant strain rate of 10^{-3} s^{-1} . The Young's modulus (E) was calculated from the slope of the initial linear portion of the stress vs. strain curve. Elongation to break was also measured.

2.4 Degradation Studies

2.4.1 Accelerated Degradation

PolyHIPEs 2 and 8 (Table 1) were tested for evidence of degradation. Small pieces of polyHIPE of known mass were placed in each well of a 24 well cell culture plate and each well was filled with 0.1M NaOH(aq) solution. The plate was then placed in an oven and maintained at 37°C for a 7 week period. At weekly time points samples were taken, washed in deionised water and acetone, then left to air dry until constant mass and the mass taken. This was repeated three times per time point. The percentage mass loss was calculated from $((\text{original mass} - \text{final mass}) / \text{original mass}) \times 100\%$.

2.4.2 Degradation under Cell Culture Conditions

This method is based on work of Baker et al.⁴⁹ Small pieces of polyHIPE 2 of known mass were sterilised in 70% (v/v) ethanol solution for three hours. The polyHIPE was then washed three times in sterile distilled water and once in Dulbecco's Modified Eagle's Medium (DMEM) containing 5% (v/v) fetal bovine serum. All subsequent processes were carried out in a sterile environment. The polyHIPEs were placed in a 24 well plate and immersed in 2 ml of medium containing penicillin and anti-fungus. The plate was then incubated at 37°C for a 15 week period. The pH of the medium was monitored during the course of the study. At weekly time points polyHIPE samples were removed, washed in sterilised deionised water before being air dried to a constant mass. The percentage weight loss, calculated as in section 2.4.1, was used to measure rate of degradation.

2.5 Cell Culture

PolyHIPE 8 (Table 1) was formed in a cylindrical mould with a diameter of 20 mm and a depth of 40 mm secured between two glass plates. It was sliced into 1 mm thick discs using a razor blade, then the discs were washed twice in acetone for two hours each time before being dried under vacuum. The discs were then placed in a 12 well plate alongside an Alvetex® control scaffold. The scaffold discs were secured using plastic clips and sterilised with 70% ethanol for 15 minutes. The ethanol was then removed and the scaffolds were washed twice with 3 ml of phosphate buffered saline (PBS). Immortalised human keratinocytes (HaCaT cells) in 0.1 ml of DMEM were placed in the centre of the well and the plates were left for 15 minutes in an incubator at 37.5 °C. A further 3 ml of DMEM was placed in each well and then the plates were left in the incubator at 37.5 °C for the specified time periods (7 and 11 days). The medium was changed every two days.

At each time period an MTT assay on three repeats of each scaffold was performed. The scaffolds were washed in PBS and placed in a clean well with the MTT reagent; 3-(4,5-dimethylthiazol-2-yl)-2,5-diphenyltetrazolium bromide (1 ml, Sigma). The well plate was covered in aluminium foil and placed in the incubator for 1 hour. The scaffolds were washed in acidified isopropanol and stirred at 100 rpm on a plate stirrer for 10 minutes. 20 µl of each solution was placed in a well in a 96 well plate with 180 µl of isopropanol. The plate was then placed in the spectrophotometer and the absorbance was detected at 570 nm.

For histology the cultured scaffold was washed three times with PBS (2ml) and fixed using Bouins solution for 48 hours. The scaffold was then washed three times using PBS (2ml) and placed in 30% ethanol solution (2ml) for 15 minutes. The cultured scaffolds were dehydrated further using 50%, 70%, 80%, 90%, 95% and 100% ethanol solution leaving for 15 minutes each time. The ethanol was removed and the scaffolds are placed in 15 ml of HistoClear for 15 minutes before 15 ml of paraffin wax was added. The scaffolds were incubated in the wax at 60°C for 30-60 minutes. The polymer was transferred to plastic embedding moulds with more molten wax and was left to set overnight. The hardened wax block was placed on a microtome and sliced (10-20 μ m). The sections were transferred to the slide bath and mounted onto a microscope slide. The slides were dried overnight.

To stain, the slides were deparaffinised in HistoClear for 5 minutes before being transferred to 100% ethanol. The slides were rehydrated in 95% and 70% ethanol and distilled water for 1 minute each time. The slides were stained in Mayers Haematoxylin solution for 5 minutes and washed in distilled water. The nuclei were stained blue with alkaline alcohol (ammonia:70% ethanol, 3:97) and dehydrated in 70% and 90% ethanol leaving for 30 seconds each time. The slides were then stained in Eosin (30 seconds) and further dehydrated in 95% and 100% ethanol. The slides were then placed twice in HistoClear for 3 minutes before having a cover slip placed on top. The slides were then viewed using a light microscope.

3. Results and Discussion

3.1 Preparation, Morphology and Mechanical Properties of Emulsion-templated Porous Thiol-Ene polyHIPEs

The monomer trimethylolpropane tris(3-mercaptopropionate) (trithiol, **1**) was reacted with two different multifunctional acrylates, trimethylolpropane triacrylate (TMPTA, **2**) and dipentaerythritol penta/hexa-acrylate (DPEHA, **3**) to produce materials with different crosslink densities and mechanical properties. DPEHA is a commercially available mixture of the penta- and hexa-acrylates in a molar ratio of 59:41. Two nominal porosities were used (80 and 90%) and emulsions were prepared with aqueous phases temperatures of 23 or 80°C (the higher temperature has been shown to produce larger void diameters which are more likely to be suitable for tissue engineering applications⁴⁶).

The influence of the aqueous phase temperature on void diameter was investigated by scanning electron microscopy (SEM) on fracture surfaces. Void diameter distributions were determined by analysis of SEM images employing a statistical correction factor to provide accurate values⁵⁰. Mean void diameter values ($\langle D \rangle$) are given in Table 1. It was found that increasing the temperature from 23 to 80°C of 80% porous trithiol-TMTPA materials produces noticeably larger voids (Figure 1a, b) and a much higher $\langle D \rangle$ value as determined by image analysis (Table 1). Interestingly, increasing the aqueous phase temperature of 90% porous materials of analogous composition does not produce a noticeable change in void diameter by SEM

(Figure 1c, d) and only a small increase by image analysis (Table 1, entries 3 and 4). The higher functionality acrylate monomer DPEHA similarly leads to a strong influence of temperature on void diameter at 80% porosity (Figure 1e-f and Table 1, entries 5 and 6). At 90% porosity, the higher temperature aqueous phase promotes a higher void diameter but, as with the TMTPA materials, the difference is less than at 80%. We speculate that the smaller influence of aqueous phase temperature on $\langle D \rangle$ at higher porosity is due to two effects: i) the inherent lower stability of the 90% internal phase volume (PV) HIPEs from which these materials are made, which increases the $\langle D \rangle$ values of the materials produced at lower temperature, relative to the 80% porosity materials (Table 1, entries 3 and 7 versus 1 and 5); ii) the higher PV HIPEs have higher viscosity, which opposes the emulsion breakdown processes that lead to higher $\langle D \rangle$ values, consequently the 90% porosity materials prepared at higher temperature have lower $\langle D \rangle$ values than the corresponding 80% porosity materials (Table 1, entries 4 and 8 versus 2 and 6). These effects combine to produce a lower difference in $\langle D \rangle$ values between samples prepared with different aqueous phase temperatures when the HIPE PV is 90%.

An important characteristic of polyHIPE materials is the mean interconnecting window diameter, $\langle d \rangle$. A suitable material for tissue engineering must be highly interconnected to allow nutrients to be transported to, and waste products removed from, the cells. The windows cannot be measured accurately from SEM images so mercury porosimetry is used. The $\langle d \rangle$ values determined by mercury porosimetry are shown in Table 1. For materials that

are sufficiently rigid to withstand the mercury intrusion process, it was observed generally that an increase in aqueous phase temperature produces a decrease in $\langle d \rangle$. In fact, the parameter that is changed most markedly is the degree of openness of the voids, expressed by $\langle d \rangle / \langle D \rangle$. As can be seen in Table 1, this is reduced in each case as temperature is increased. This is because increased temperature reduces emulsion stability, leading to polyHIPE materials that are more closed cell in nature. These results are in keeping with those of other studies of the influence of aqueous phase temperature on polyHIPE morphology⁴⁶. Suitable scaffolds for tissue engineering require highly interconnected voids with an average diameter of at least 50 μm . Figure 1 and Table 1 demonstrate that this has been achieved for the materials prepared by thiol-ene emulsion templating.

The extent of incorporation of the trithiol monomer was determined by elemental (S) analysis. In agreement with previous results, the trithiol was incorporated at between 75-88% of the level present in the HIPE. The loss of trithiol could be due to its ability to partition into the aqueous phase, or possibly because there is some acrylate homopolymerisation concurrent with thiol-ene reaction. The degree of crosslinking of the materials was investigated by solid state ^{13}C NMR spectroscopy. The integral corresponding to the C=C bond of the acrylate at ~ 130 ppm was compared to the integral for the C=O bond at ~ 170 ppm to obtain values for the extent of crosslinking. The number of residual double bonds indicates any unreacted acrylate groups and therefore the degree of cross-linking can be calculated.

The results are tabulated in Table 1 and show that the degree of crosslinking varies between 81 and 94%, similar to the elemental analysis results. This suggests that acrylate homopolymerisation is limited.

The mechanical properties of a substrate have been shown to have an influence on the ability of cells to adhere, proliferate and differentiate^{47, 51}. Trithiol-TMPTA polyHIPEs are quite flexible whereas those prepared from DPEHA are much more rigid (see videos in Supplementary Information). Consequently, it is possible that TMTPA derived scaffolds could be appropriate for soft tissue culture, whereas DPEHA materials might be more suitable for the culture of harder tissue types, such as cartilage and bone. The mechanical properties of the two scaffold types were investigated under tension. It can be seen from Figure 2 that the more highly crosslinked DPEHA polyHIPE is able to withstand a much higher load than the TMTPA material (13.62N compared to 2.14N). The Young's moduli of the materials were measured from the initial gradient of the plots in Figure 2. It was found that the DPEHA polyHIPE sample has a Young's modulus of 19.18 MPa whereas the corresponding value for the TMTPA sample is 100 times lower at 0.193 MPa. This confirms that the trithiol-DPEHA polyHIPEs are stiffer than the trithiol-TMPTA materials. Figure 2 also shows that the TMPTA samples extend much further before fracturing than the DPEHA polyHIPEs. The maximum extension of the TMTPA material before fracture is 13.2 mm, while the maximum extension of DPEHA polyHIPE before fracture is only 1.8 mm. This also demonstrates the greater flexibility of the TMTPA polyHIPEs.

3.2 *In Situ* Chemical Functionalisation

The thiol-ene photocuring process is rapid and occurs under ambient temperature conditions. This provides an opportunity to functionalise the scaffolds *in situ* by incorporating into the monomer phase molecules that possess moieties that will participate in the crosslinking reaction (alkenes, alkynes, and thiols for example). To investigate this, three molecules possessing either an acrylate or a thiol group were chosen: fluorescein *o*-acrylate; 1,1,1,3,3,3-hexafluoroisopropyl acrylate (HFiPA); and 2,2,2-trifluoroethanethiol (fluorothiol). Fluorescein *o*-acrylate is a highly conjugated fluorescent molecule, and thus its incorporation into polyHIPE materials can be demonstrated qualitatively by illumination with UV light. The fluorinated acrylate and thiol introduce multiple fluorine atoms into the scaffold which can be quantified by elemental analysis.

The fluorescent acrylate was added to a 90% PV HIPE containing DPEHA (equivalent to polyHIPE 8 in Table 1), at levels of 1 and 2 mol% of the total amount of acrylate groups present (the 1:1 stoichiometry of thiol:acrylate was maintained). The resulting materials were cut and the cross-sections examined under illumination with a low power UV lamp (Figure 3). The fluorescent molecule has clearly been incorporated into the scaffold, and the extent of incorporation appears to be dose dependent. The morphology of the polyHIPE material is unaffected by the incorporation of the fluorescent molecule (see Supplementary Information, Figure S1).

The fluorinated molecules were used to prepare polyHIPEs with a composition corresponding to that of polyHIPE 7 in Table 1. Each molecule was added at different levels (mol % of acrylate or thiol content) and the 1:1 acrylate to thiol stoichiometry was maintained. Table 2 shows that the fluorinated acrylate can be incorporated successfully into the polyHIPE at a level of between 60 and 90% of the amount added to the precursor HIPE. The fluorinated thiol functionalises the polyHIPE significantly less at 30% of the expected value. This is possibly because the fluorinated thiol is partially water-soluble; it has a log P value of 1.6, whereas the fluorinated acrylate has a log P value of 3.0. Because the fluorinated thiol is partially soluble in the aqueous phase, it can partition out of the oil phase before polymerisation occurs and thus the observed fluorine content is lower than expected.

3.3 Degradation Studies

Scaffolds for tissue engineering applications are required to be biodegradable, consequently we undertook experiments to determine the extent and rate of degradation under different conditions. Accelerated degradation studies using 1M and 0.1M NaOH(aq) solutions at 37°C were initially performed. It was found that the 1M NaOH(aq) solution degraded the polyHIPE sample completely within 48 hours. In 0.1M NaOH(aq) solution, degradation of both an 80% porous trithiol-TMPTA polyHIPE (polyHIPE 2) and a 90% porous trithiol-DPEHA polyHIPE (polyHIPE 8) was carried out over 7 weeks. Figure 4a shows the mass loss of the polyHIPE samples over the 7 week period.

PolyHIPE 2 degrades steadily with a mean final percentage mass loss of 20%. PolyHIPE 8 has a very steep initial mass loss to around 30%. Degradation then appears to slow down and by 6 weeks has not changed significantly. PolyHIPE 8 degrades to a higher extent than polyHIPE 2 most probably because it is of higher porosity, so there is better access of the solution to the surface. Also, DPEHA has more ester linkages than TMPTA and so it has more sites for degradation.

The SEM images of polyHIPE 2 before and after immersion in 0.1M NaOH(aq) solution for 7 weeks are also shown in Figure 4 (b and c). Small holes are seen around the interconnecting windows between voids in the degraded samples, indicating hydrolysis and mass loss. The degradation evidence appears in this location because this is the thinnest part of the polyHIPE polymer phase. Further degradation studies were conducted under typical cell culture conditions. The rate of scaffold degradation in cell culture medium at 37°C in an incubator was assessed for polyHIPE 2 over a 15 week period (Figure 5). Degradation occurs much more gradually than in the 0.1M NaOH(aq) solution. After 15 weeks it was found that the mean mass loss was 19%. This clearly indicates the ability of these porous materials to degrade under typical *in vitro* cell culture conditions. The degradation rate is in the same range as amorphous poly(lactic acid) (PLA), a commonly used biomaterial for tissue engineering. Depending on molecular weight, PLA is reported to have a degradation (mass loss) half-life of 10-110 weeks in phosphate-buffered saline (PBS) at 37°C⁵².

3.4 Cell culture

In vitro cell culture experiments were undertaken to assess the biocompatibility, and therefore suitability as a scaffold for tissue engineering, of these novel thiol-ene polyHIPE materials. Immortalised human keratinocytes (HaCaTs) were cultured *in vitro* on polyHIPE 8 and on a commercially available polystyrene-based polyHIPE 3D cell culture scaffold (Alvetex®) as a positive control, for up to 11 days. Figure 6a demonstrates successful culture of HaCaTs on both polyHIPE 8 and on the Alvetex control. Viability was assessed using an MTT assay, in which a yellow tetrazole is metabolised by living cells into a purple formazan. The formazan dye is quantified by UV-vis spectrophotometry, giving a measure of metabolic activity and therefore cell viability. For both scaffolds absorbance increases with time, which relates directly to cell proliferation. Although cell viability on the thiol-ene polyHIPE scaffold is lower than control at both time points, the experiments demonstrate the ability of these scaffolds to support cell growth and consequently gives an indication of scaffold biocompatibility. Results from histology experiments on cells cultured on the thiol-ene scaffold are shown in Figure 6b and c. At day 7, cell growth on the surface is clearly seen however penetration into the scaffold is limited (cells are stained to allow visualisation). Some evidence of cell in-growth is seen at the later time point (day 11; Figure 6c). Further work is underway to explore in more detail the biocompatibility of these scaffolds using other cell types, and to probe the influence of scaffold mechanical properties on cell behaviour.

4. Conclusions

Thiol-ene photopolymerisation has been used to produce porous polymeric materials (polyHIPEs) suitable for tissue engineering from multifunctional acrylates and thiols. It was found that increasing the temperature of the aqueous phase from 23 to 80 °C produced an increase in the mean void diameter, and that the extent of this increase was dependent on porosity. The mechanical properties of the polyHIPE can be controlled by altering the functionality of the acrylate component. A tri-acrylate produces a material with a low modulus (0.19 MPa) while a mixture of penta- and hexa-acrylates produces a material with a modulus around 100 times higher. The polyHIPEs can be functionalised *in situ* using functional acrylates or thiols. This was demonstrated using a fluorescent acrylate, a fluorinated acrylate and a fluorinated thiol. Degradation of the materials in NaOH solution occurred at a rate depending on hydroxide ion concentration, and was also shown to proceed to 19% mass loss after 15 weeks in cell culture medium at 37°C. Immortalised human keratinocytes were successfully cultured on thiol-ene polyHIPEs, indicating that they are biocompatible. Cell growth was mainly on the surface of the scaffold and penetration was limited. Overall, it has been shown that the thiol-ene polyHIPEs are potentially suitable materials for tissue engineering. Further work will explore the growth of other cell types on these materials, with a view to preparing optimised scaffolds for particular cell types.

Acknowledgements

Durham University is thanked for funding. The "Precision Polymer Materials" RNP programme from the European Science Foundation is also acknowledged. Solid state NMR spectroscopy was conducted using the EPSRC Solid State NMR National Facility at Durham University.

References

1. D. Barby and Z. Haq, *EP Pat.*, 60138, 1982.
2. N. R. Cameron, *Polymer*, 2005, **46**, 1439-1449.
3. N. R. Cameron, P. Krajnc and M. S. Silverstein, in *Porous Polymers*, eds. M. S. Silverstein, N. R. Cameron and M. A. Hillmyer, Wiley & Sons, Hoboken, N.J., 2011, pp. 119-172.
4. N. R. Cameron and D. C. Sherrington, *Adv. Polym. Sci.*, 1996, **126**, 163-214.
5. S. D. Kimmins and N. R. Cameron, *Adv. Funct. Mater.*, 2011, **21**, 211-225.
6. H. F. Zhang and A. I. Cooper, *Soft Matter*, 2005, **1**, 107-113.
7. K. J. Lissant (ed.), *Emulsions and Emulsion Technology Part 1*, Marcel Dekker Inc., New York, 1974.
8. J. M. Williams, *Langmuir*, 1988, **4**, 44-49.
9. N. R. Cameron, D. C. Sherrington, I. Ando and H. Kurosu, *J. Mater. Chem.*, 1996, **6**, 719-726.
10. P. W. Small and D. C. Sherrington, *Chem. Commun.*, 1989, 1589-1591.

11. A. Barbetta, N. R. Cameron and S. J. Cooper, *Chem. Commun.*, 2000, 221-222.
12. P. Krajnc, J. F. Brown and N. R. Cameron, *Org. Lett.*, 2002, **4**, 2497-2500.
13. K. Jerabek, I. Pulko, K. Soukupova, D. Stefanec and P. Krajnc, *Macromolecules*, 2008, **41**, 3543-3546.
14. N. R. Cameron and D. C. Sherrington, *J. Mater. Chem.*, 1997, **7**, 2209-2212.
15. A. K. Hebb, K. Senoo, R. Bhat and A. I. Cooper, *Chem. Mat.*, 2003, **15**, 2061-2069.
16. N. Leber, J. D. B. Fay, N. R. Cameron and P. Krajnc, *J. Polym. Sci. Pt. A: Polym. Chem.*, 2007, **45**, 4043-4053.
17. S. Kovacic, K. Jerabek and P. Krajnc, *Macromol. Chem. Phys.*, 2011, **212**, 2151-2158.
18. R. Butler, C. M. Davies and A. I. Cooper, *Adv. Mater.*, 2001, **13**, 1459-1463.
19. H. F. Zhang, I. Hussain, M. Brust and A. I. Cooper, *Adv. Mater.*, 2004, **16**, 27-30.
20. B. Tan, J. Y. Lee and A. I. Cooper, *Macromolecules*, 2007, **40**, 1945-1954.
21. N. R. Cameron and D. C. Sherrington, *Macromolecules*, 1997, **30**, 5860-5869.
22. H. Deleuze, R. Faivre and V. Herroquez, *Chem. Commun.*, 2002, 2822-2823.

23. E. M. Christenson, W. Soofi, J. L. Holm, N. R. Cameron and A. G. Mikos, *Biomacromolecules*, 2007, **8**, 3806-3814.
24. S. Kovacic, P. Krajnc and C. Slugovc, *Chem. Commun.*, 2010, **46**, 7504-7506.
25. S. Kovacic, K. Jerabek, P. Krajnc and C. Slugovc, *Polym. Chem.*, 2012, **3**, 325-328.
26. A. Barbetta, M. Dentini, M. S. De Vecchis, P. Filippini, G. Formisano and S. Caiazza, *Adv. Funct. Mater.*, 2005, **15**, 118-124.
27. A. Barbetta, M. Dentini, E. M. Zannoni and M. E. De Stefano, *Langmuir*, 2005, **21**, 12333-12341.
28. A. Barbetta, M. Massimi, L. C. Devirgiliis and M. Dentini, *Biomacromolecules*, 2006, **7**, 3059-3068.
29. S. J. Pierre, J. C. Thies, A. Dureault, N. R. Cameron, J. C. M. van Hest, N. Carette, T. Michon and R. Weberskirch, *Adv. Mater.*, 2006, **18**, 1822-1826.
30. D. Cummins, P. Wyman, C. J. Duxbury, J. Thies, C. E. Koning and A. Heise, *Chem. Mat.*, 2007, **19**, 5285-5292.
31. D. M. Cummins, P. Magusin and A. Heise, in *Controlled/Living Radical Polymerization: Progress in ATRP*, 2009, vol. 1023, pp. 327-341.
32. E. Lovelady, S. D. Kimmins, J. J. Wu and N. R. Cameron, *Polym. Chem.*, 2011, **2**, 559-562.
33. A. Barbetta, M. Massimi, B. Di Rosario, S. Nardecchia, M. De Colli, L. C. Devirgiliis and M. Dentini, *Biomacromolecules*, 2008, **9**, 2844-2856.
34. M. Bokhari, M. Birch and G. Akay, *Adv. Exper. Med. Biol.*, 2003, **534**, 247-254.

35. M. A. Bokhari, G. Akay, S. Zhang and M. A. Birch, *Biomaterials*, 2005, **26**, 5198-5208.
36. M. A. Bokhari, G. Akay, S. G. Zhang and M. A. Birch, *Biomaterials*, 2005, **26**, 5198-5208.
37. W. Busby, N. R. Cameron and C. A. B. Jahoda, *Biomacromolecules*, 2001, **2**, 154-164.
38. W. Busby, N. R. Cameron and C. A. B. Jahoda, *Polym. Int.*, 2002, **51**, 871-881.
39. R. S. Moglia, J. L. Holm, N. A. Sears, C. J. Wilson, D. M. Harrison and E. Cosgriff-Hernandez, *Biomacromolecules*, 2011, **12**, 3621-3628.
40. Y. Lumelsky and M. S. Silverstein, *Macromolecules*, 2009, **42**, 1627-1633.
41. Y. Lumelsky, I. Lalush-Michael, S. Levenberg and M. S. Silverstein, *J. Polym. Sci. Pt. A: Polym. Chem.*, 2009, **47**, 7043-7053.
42. M. Bokhari, R. J. Carnachan, N. R. Cameron and S. A. Przyborski, *Biochem. Biophys. Res. Commun.*, 2007, **354**, 1095-1100.
43. M. Bokhari, R. J. Carnachan, N. R. Cameron and S. A. Przyborski, *J. Anatomy*, 2007, **211**, 567-576.
44. M. W. Hayman, K. H. Smith, N. R. Cameron and S. A. Przyborski, *Biochem. Biophys. Res. Commun.*, 2004, **314**, 483-488.
45. M. W. Hayman, K. H. Smith, N. R. Cameron and S. A. Przyborski, *J. Biochem. Biophys. Methods*, 2005, **62**, 231-240.
46. R. J. Carnachan, M. Bokhari, S. A. Przyborski and N. R. Cameron, *Soft Matter*, 2006, **2**, 608-616.

47. D. E. Discher, P. Janmey and Y.-L. Wang, *Science*, 2005, **315**, 1139-1143.
48. <http://rsbweb.nih.gov/ij/>.
49. S. C. Baker, G. Rohman, J. Hinley, J. Stahlschmidt, N. R. Cameron and J. Southgate, *Macromol. Biosci.*, 2011, **11**, 618-627.
50. A. Barbetta and N. R. Cameron, *Macromolecules*, 2004, **37**, 3188-3201.
51. A. J. Engler, S. Sen, H. L. Sweeney and D. E. Discher, *Cell*, 2006, **126**, 677-689.
52. S. Li, in *Scaffolding in Tissue Engineering*, eds. P. X. Ma and J. Elisseeff, Taylor & Francis, Boca Raton, 2006.

Table 1. Thiol-ene PolyHIPE Characterisation Data

PolyHIPE ^a	T _{aq} ^b (°C)	Porosity (%)	<D> ^c (μm)	<d> ^d (μm)	<d>/<D>	[S] ^e (%)	X ^h (%)
1	23	80	44.0	N/A	N/A	11.35 ^f	89
2	80	80	91.5	N/A	N/A	11.75 ^f	81
3	23	90	54.3	18.1	0.33	10.84 ^f	94
4	80	90	67.3	15.6	0.24	11.76 ^f	83
5	23	80	34.2	9.0	0.26	12.35 ^g	89
6	80	80	125	13.5	0.11	12.19 ^g	90
7	23	90	45.4	31.3	0.69	10.64 ^g	92
8	80	90	108	18.4	0.17	11.64 ^g	89

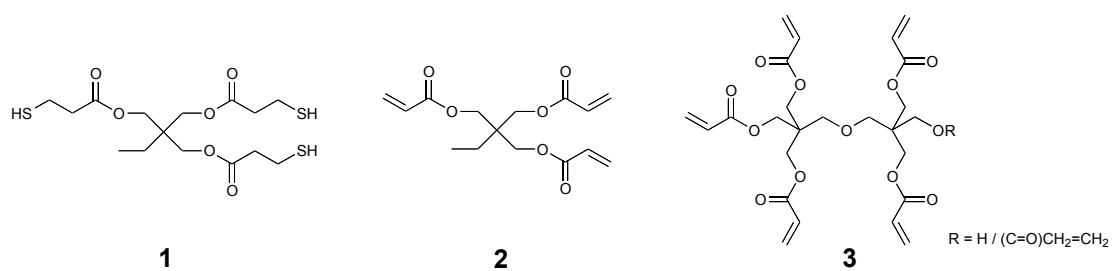
^a PolyHIPEs 1-4 prepared with TMPTA, polyHIPEs 5-8 prepared with DPEHA;

^b aqueous phase temperature; ^c mean void diameter determined by SEM; ^d mean window diameter determined by Hg porosimetry; ^e sulfur content determined by elemental analysis; ^f theoretical sulfur content = 13.84%; ^g theoretical sulfur content = 14.04%; ^h degree of crosslinking determined by ¹³C solid state NMR spectroscopy.

Table 2. Fluorine Analysis of *In Situ* Functionalised Thiol-ene polyHIPEs

Fluorinated molecule ^a	Theoretical Fluorine Content (%)	Observed Fluorine Content ^b (%)
HFiPA	0.98	0.90
HFiPA	2.43	1.48
HFiPA	4.99	3.43
Fluorothiol	0.98	0.26
Fluorothiol	1.96	0.68

^a HFiPA = 1,1,1,3,3,3-hexafluoroisopropyl acrylate, Fluorothiol = 2,2,2-trifluoroethanethiol; ^b Determined by elemental analysis.



Scheme 1. Monomers used to prepare thiol-ene polyHIPE materials.

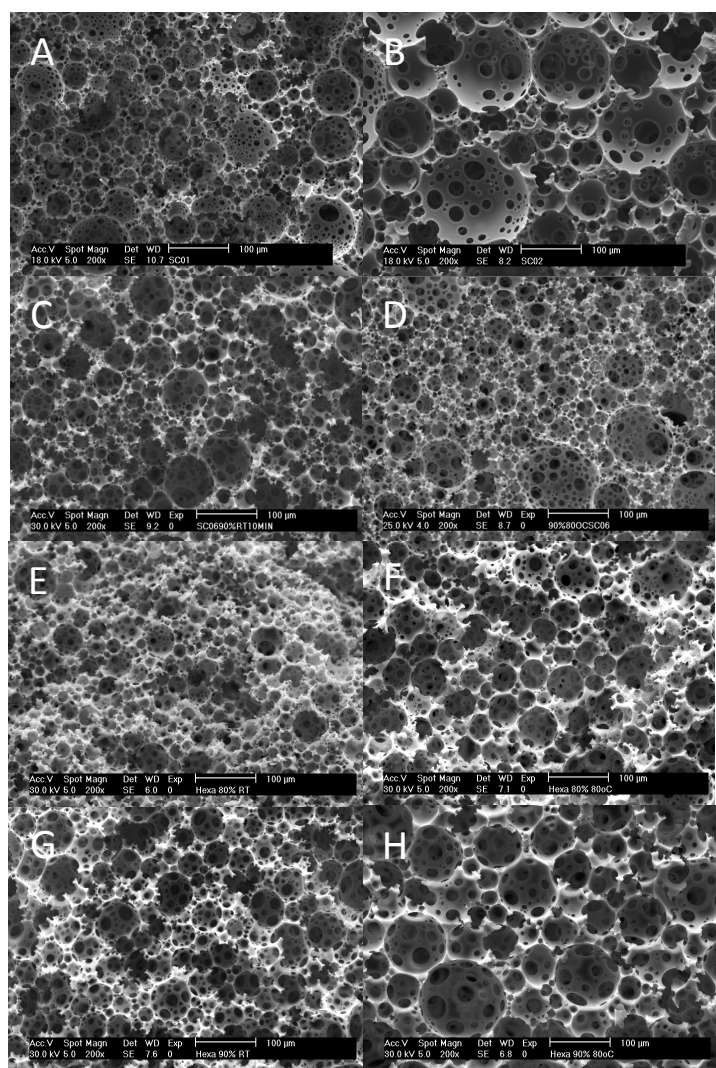


Figure 1. SEM images of trithiol-TMTPA and -DPEHA polyHIPEs: A) to G), polyHIPEs 1-8 (see Table 1 for polyHIPE compositions).

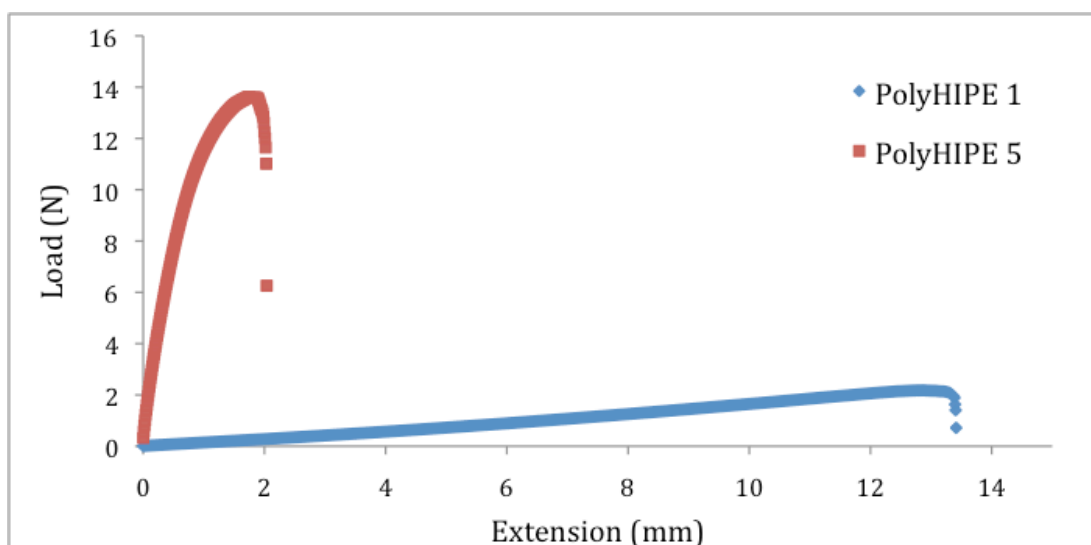


Figure 2. Mechanical testing results for 80% porous trithiol-TMPTA polyHIPE (polyHIPE 1, diamonds) and 80% porous trithiol-DPEHA polyHIPE (polyHIPE 5, squares).

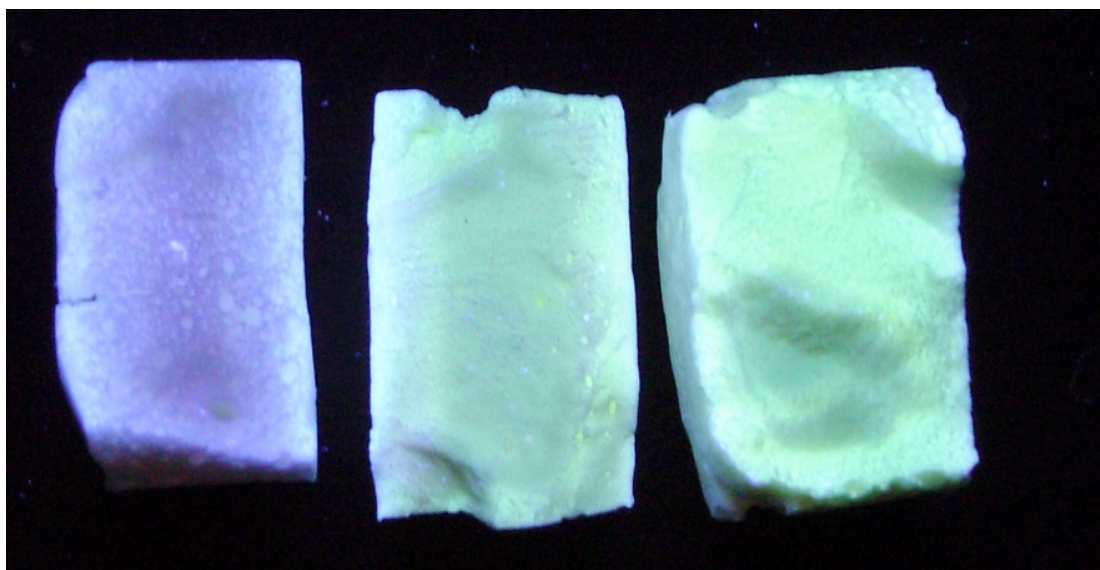


Figure 3. PolyHIPE 8 functionalised with fluorescein *o*-acrylate, illuminated under UV light. Left: unfunctionalised material; Middle: functionalised with fluorescein *o*-acrylate at 1 mol% of the acrylate group content; Left: functionalised with fluorescein *o*-acrylate at 2 mol% of the acrylate group content.

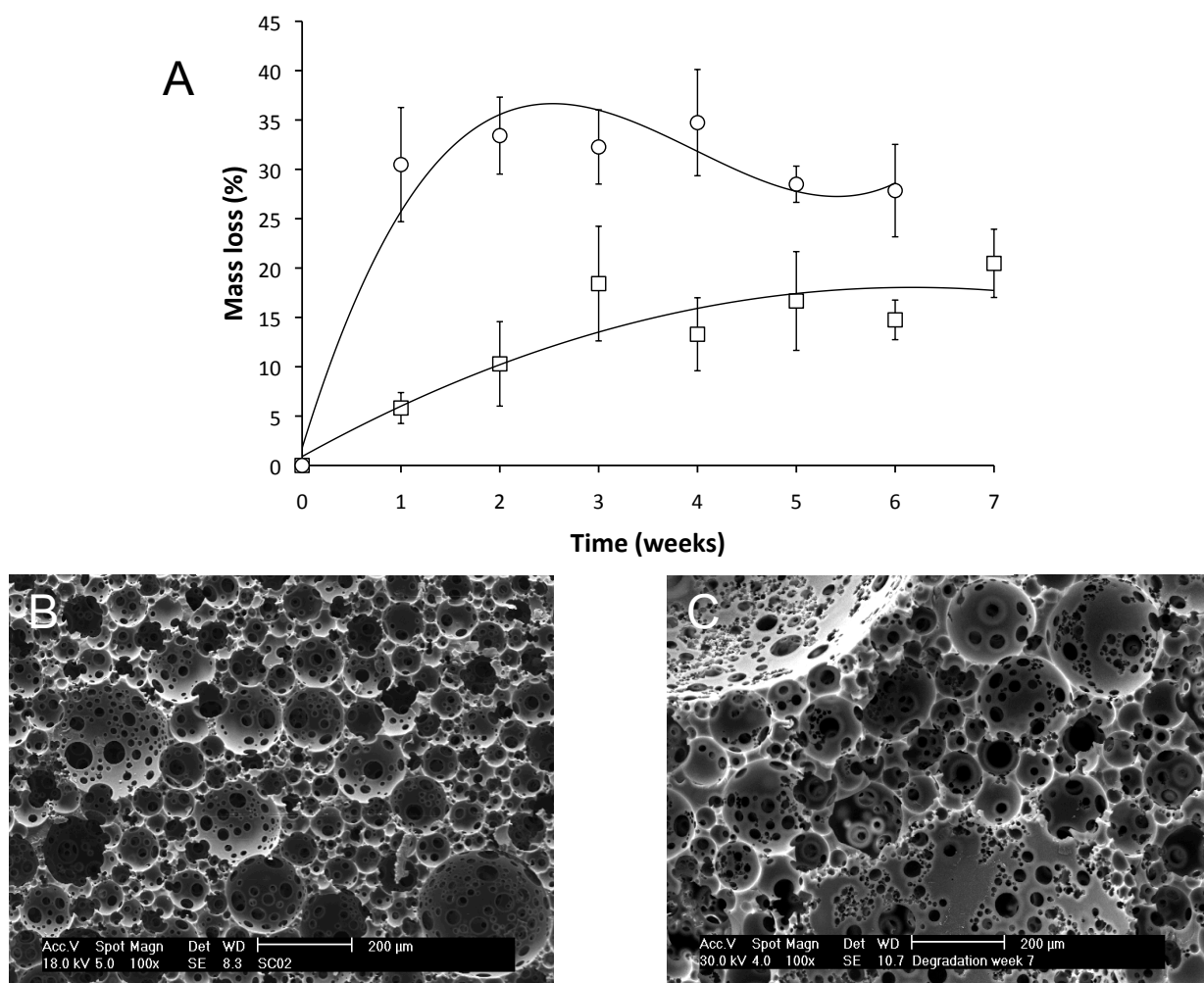


Figure 4. (A) rate of degradation of polyHIPE 2 (squares) and polyHIPE 8 (circles) plotted as percentage mass loss against time (error bars show standard deviation of the mean); (B) and (C) SEM images of polyHIPE 2 at various degradation time points: (B) week 0, (C) week 7.

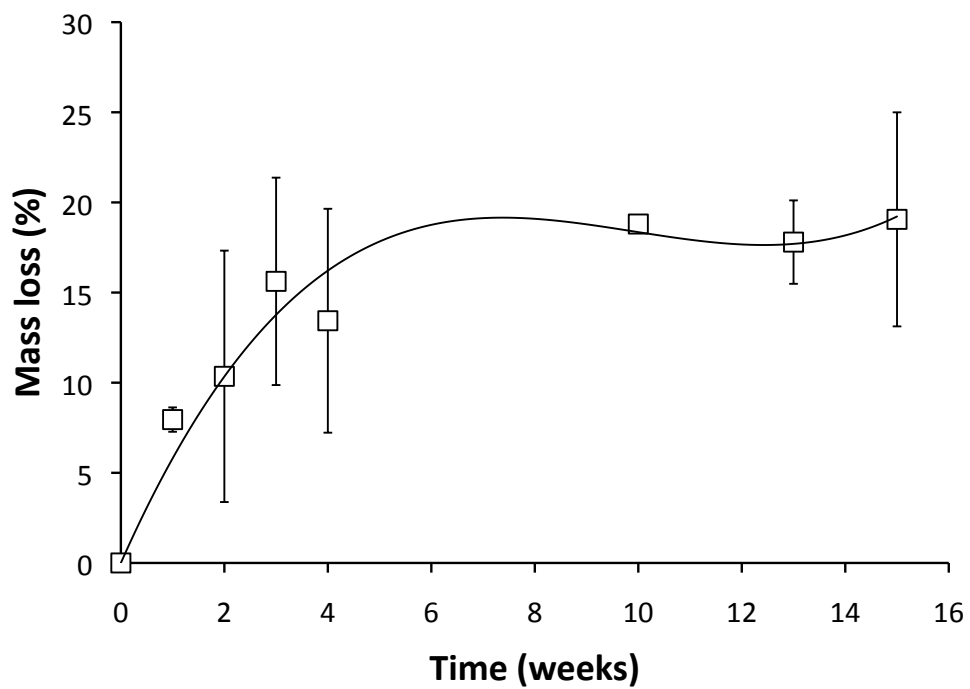


Figure 5. Degradation of polyHIPE 2 in cell culture medium at 37°C, plotted as percentage weight loss against time (error bars show standard deviation of the mean).

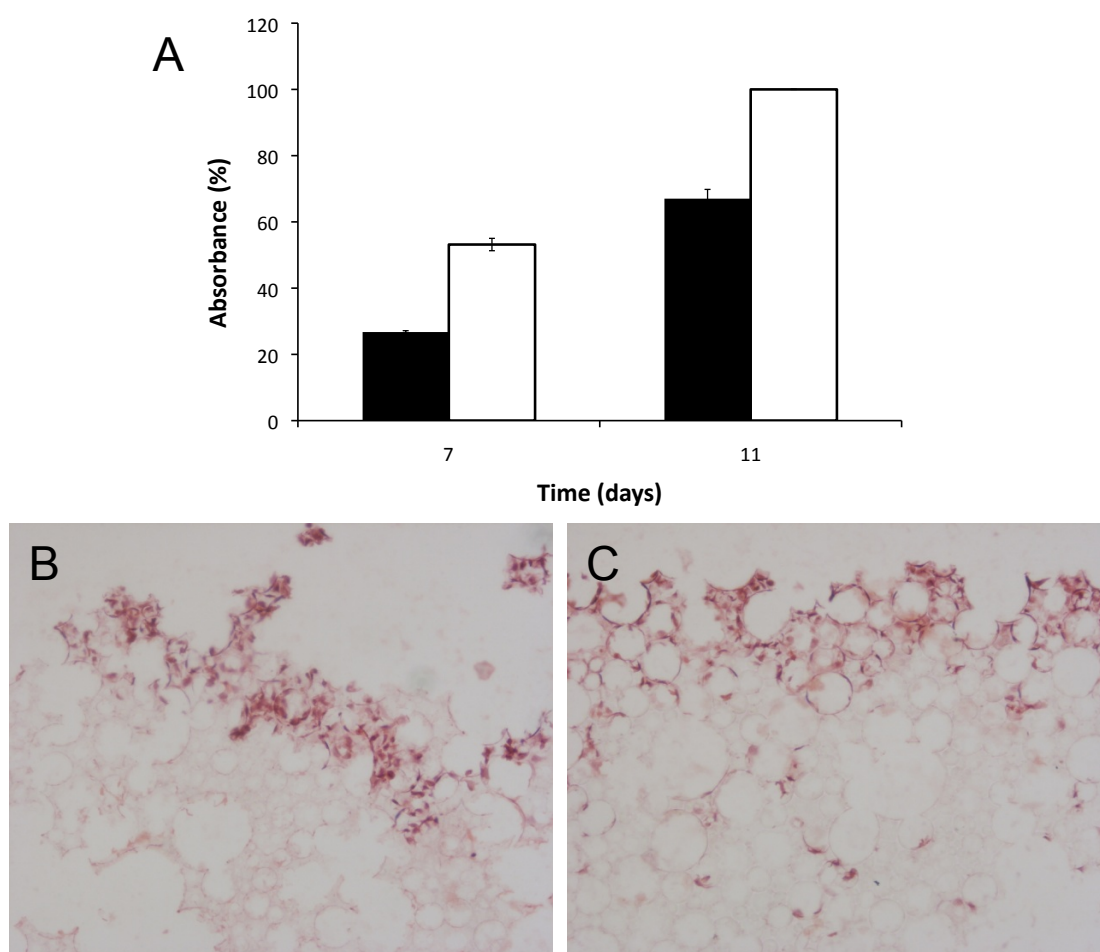


Figure 6. (A) Viability of HaCaT cells cultured on polyHIPE 8 (black) and Alvetex® control (white) scaffolds shown as a plot of absorbance against time (error bars show standard deviation of the mean); (B) and (C) histology images of HaCaT cell growth on polyHIPE 8 for different time periods: (B) 7 days, (C) 11 days. Magnification $\times 100$.